Monitoring of Land Cover Changes between 1990 and 2014 Over Cyprus Using Multi-Temporal Landsat Imagery

Burcu Kurtoğlu Erkmen[*] [iD], **Hakan Yener** [iD]

Istanbul University - Cerrahpasa, Faculty of Forestry, Forest Engineering Department, 34473 Istanbul, Türkiye

Abstract

Determining changes in forest resources and land cover/land use is crucial for sustainable forest planning. This study aims to determine changes in land cover classes, including forest areas, agricultural areas, settlement areas, other non-forest areas, and water bodies in the study area located in Cyprus between 1990 and 2014. The study utilized digital management plans, a high-resolution base map, and Landsat satellite images for the relevant years. Necessary preprocessing steps were applied to prepare the satellite data for classification. Initially, unsupervised classification was conducted on the images to determine the number of distinguishable sub-information classes. Subsequently, supervised classification was performed using the maximum likelihood algorithm with the provision of training areas. The sub classes generated based on the supervised classification were consolidated into five main classes. After the classification process, the accuracy of the classification for each image was determined. Accordingly, the overall classification accuracy of the map from the 1990 Landsat 5 TM satellite image was 92%, with 0.90 Kappa Statistics. The overall classification accuracy of the map from 2014 Landsat 8 OLI satellite image was 89.20%, with 0.87 Kappa statistics. Then, land cover change analysis was conducted to compare a twenty-four-year period within the study area.

Keywords: Remote sensing, Change analysis, Post-classification comparison method, Image classification, Forestry

1. Introduction

Spatio-temporal determination of forest resources is crucial for sustainable forest management and planning. Remote Sensing (RS), in conjunction with geographic information Science (GIS), offers an effective and innovative approach to rapidly detect the spatial structural characteristics of forest and natural resources and their surroundings (Koç and Selik, 2004; Yener and Koç, 2006). Numerous studies have been conducted on land use land cover classification (LULCC) and change detection employing different methods along with different RS data sources. A study by Berberoglu and Akin (2009) detected land cover/land use changes in the Mediterranean region using Landsat TM images for three different periods (1985, 1993, and 2005). Four different change detection techniques were applied, and object-based supervised classification was employed as a cross-classification approach to determine 'from–to' changes, allowing for the evaluation of all four methods. The results indicated that change vector analysis achieved the highest overall accuracy of 75.25% for the 1985–1993 period and 75.55% for the 1993–2005 period-for the Mediterranean region.

Mas (1999) conducted a study to determine LULC and changes in the Terminos Lagoon region (Mexico) using Landsat Multispectral Scanner (MSS) images from different periods. Six change detection methods were employed, including image differencing, vegetative index differencing, selective principal components analysis (SPCA), direct multi-date unsupervised classification, post-classification differencing, and a combination of image enhancement and post-classification comparison. The accuracy assessment was conducted for the change detection results obtained from the six methods. Ultimately, the results noted that the post-classification comparison method provides the highest overall accuracy of 86.87% and a kappa value of 0.6191.

Sunar (1998) analyzed land cover change and the significant development pressure on the environment in Ikitelli, Istanbul. Four different change detection methods were used: image overlay, image differencing, principal components analysis and post-classification comparison. Landsat TM images acquired in for two different periods (1984, 1992). It was noted that image overlay and image differencing methods were easily applicable, while classified images through principal

components analysis highlighted differences attributable to change. Each of the change detection methods possessed certain values concerning ease, information content, and interpretability.

There is a wide variety of alternatives for the combination of change detection methods and classification procedures, all of which possess varying degrees of flexibility and validity (Lu et al., 2004). Each change detection method has different merits, and a single approach is not optimal for all situations (Lu et al., 2004). In this study, the post-classification comparison method was used to determine land use land cover classification and change detection. The post-classification comparison method is a commonly used quantitative change detection method. In this technique, which necessitates the classification and accuracy assessment of each remotely sensed image, the images are compared pixel by pixel using a change matrix (Jensen, 1996). While some techniques only provide information on whether change has occurred or not, the greatest advantage of the post-classification comparison method is its ability to provide a complete matrix of change directions (Lu et al., 2004).

To perform such spatio-temporal analysis, satellite imagery with consistent temporal coverage and wide accessibility is required. Satellite images, which provide a rapid and effective data collection method over large areas, were utilized (Yener and Koç, 2006). The data transmitted by the Landsat satellite are received and archived by ground stations, thereby enabling the temporal analysis of land surface changes through remote sensing techniques. The availability of archived imagery, thanks to the wide spatial coverage, consistent data characteristics, and relatively low cost of satellite images, has made Landsat data a widely used source in scientific research related to natural resources (Çoban, 2006). Data from the TM sensor are utilized in various applications, including resource management, mapping, environmental monitoring, and change detection (CCRS, 2009). The OLI sensor is useful for approaches to land cover, condition, disturbance monitoring, and change determination, as well as for large-area land cover monitoring and mapping applications (Roy et al., 2014).

The primary aim of this study is to detect and analyze land cover changes that occurred between 1990 and 2014 in the designated study area on the island of Cyprus. The findings of the study are also expected to contribute to research and decision-making processes concerning forest resources and land management in the region.

2. Materials and Methods
2.1. Study Area and Data

With a total area of 9251 km², Cyprus is the third largest island in the Mediterranean after Sicily and Sardinia. The study area covers approximately 3,242 km² of the island of Cyprus, situated between the north latitudes of 34° 33′ - 35° 42′ and east longitudes of 32° 16′ - 34° 36′ (Figure 1). It is anticipated that factors such as population growth and forest fires occurring in the region between 1990 and 2014 have led to changes in land use patterns.
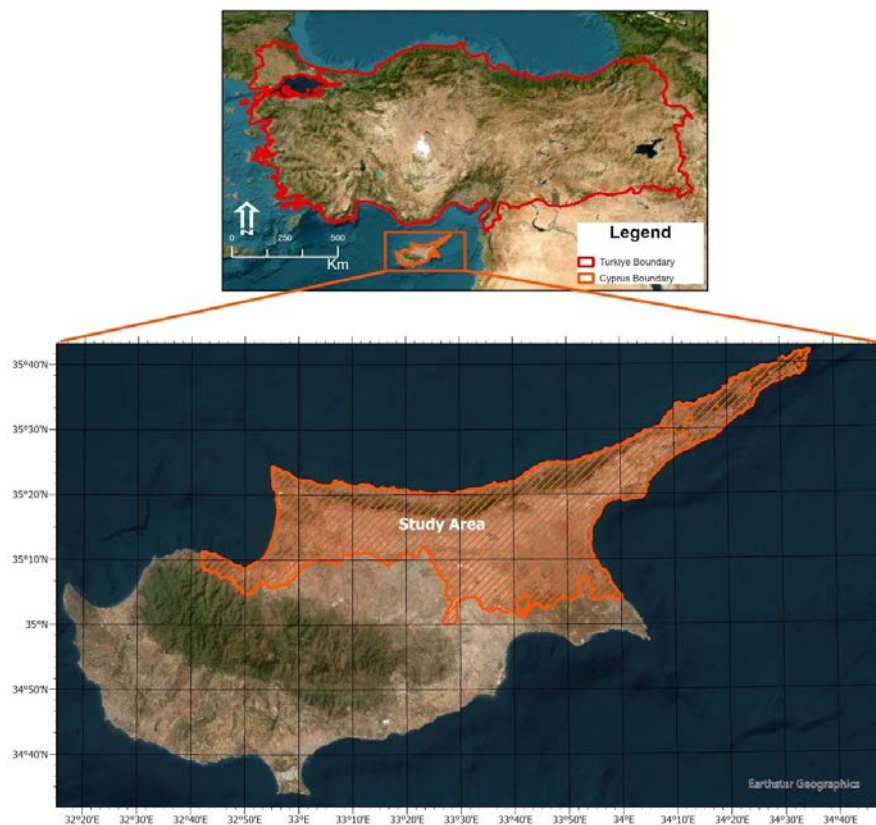

Figure 1. Study area located in the north of Cyprus

To determine the temporal changes in the study area, satellite data sets from two different dates were used (Table 1). For change detection analysis, it is recommended that there be no significant seasonal and temporal differences between the image acquisition dates. However, the dataset from 1990 covering a relatively small portion of the study area has dense cloud cover, resulting in inadequate quality. Therefore, a dataset that met the required quality standards and closely matched the nearest seasonal and temporal parameters was identified and used for classification.

Table 1. Information of the used satellite data

Landsat Satellite path and row numbers	1990 Data Landsat 5 TM	2014 Data Landsat 8 OLI
p175 r35	10.08.1987 - 07:43:25	15.08.2014 - 08:16:09
p176 r35	08.04.1990 - 07:42:16	22.08.2014 - 08:22:20
p176 r36	08.04.1990 - 07:42:40	22.08.2014 - 08:22:44

The characteristic of the sensors used in the study (TM and OLI) are provided in Table 2. To determine the forest cover and other land use land cover types and the changes between 1990 and 2014, the 6 bands of the 1990 Landsat 5 TM data set and the 7 bands of the 2014 Landsat 8 OLI data set were used. Digital forest management plans were used to identify the training areas for classifying the satellite images for both years. The high-resolution base map provided by Esri was utilized for accuracy assessments after visually comparing the classified 2014 satellite image and the base map to determine whether they were generated in the same year. These images are obtained from various providers, including satellite and aerial imagery at one-meter resolution or better for most of the world's landmass, alongside lower-resolution satellite imagery worldwide (ESRI, 2024). For this study, Erdas Imagine 2014 and ArcMap 10.1 were used.

2.2. Classification Process

Pre-classification preparatory works include layer stacking spectral bands as shown in Figure 2, mosaicking frames that constitute the study area, generating vegetation indices, and clipping images. Firstly, the spectral bands of the satellite data were combined. The 6 bands of the Landsat 5 TM images for 1990 (1, 2, 3, 4, 5, 7) and the 7 bands of the Landsat OLI images for 2014 (1, 2, 3, 4, 5, 6, 7) were combined layer, study area.

Tablo 2. Technical characteristics of TM and OLI sensors (USGS, 2024)

Satellite/ Sensor	Band number	Spectral resolution (µm)	Spatial resolution (m)	Radiometric resolution (bit)	Swath width (km)	Revisit period (day)	Band name
Landsat5/ TM	1	0.45 - 0.52	30	8	185	16	Blue
	2	0.52 - 0.60	30	8	185	16	Green
	3	0.63 - 0.69	30	8	185	16	Red
	4	0.76 - 0.90	30	8	185	16	Near Infrared (NIR)
	5	1.55 - 1.75	30	8	185	16	Shortwave Infrared (SWIR) 1
	6	10.4 - 12.5	120	8	185	16	Thermal
	7	2.08 - 2.35	30	8	185	16	Shortwave Infrared (SWIR) 2
Landsat8/ OLI TIRS	1	0.43 - 0.45	30	12	185	16	Coastal aerosol
	2	0.45 - 0.51	30	12	185	16	Blue
	3	0.53 - 0.59	30	12	185	16	Green
	4	0.64 - 0.67	30	12	185	16	Red
	5	0.85 - 0.88	30	12	185	16	Near Infrared (NIR)
	6	1.57 - 1.65	30	12	185	16	Shortwave Infrared (SWIR) 1
	7	2.11 - 2.29	30	12	185	16	Shortwave Infrared (SWIR) 2
	8	0.50 - 0.68	15	12	185	16	Panchromatic
	9	1.36 - 1.38	30	12	185	16	Cirrus
	10	10.60 - 11.19	100*	12	185	16	Thermal Infrared (TIRS) 1
	11	11.50 - 12.51	100*	12	185	16	Thermal Infrared (TIRS) 2

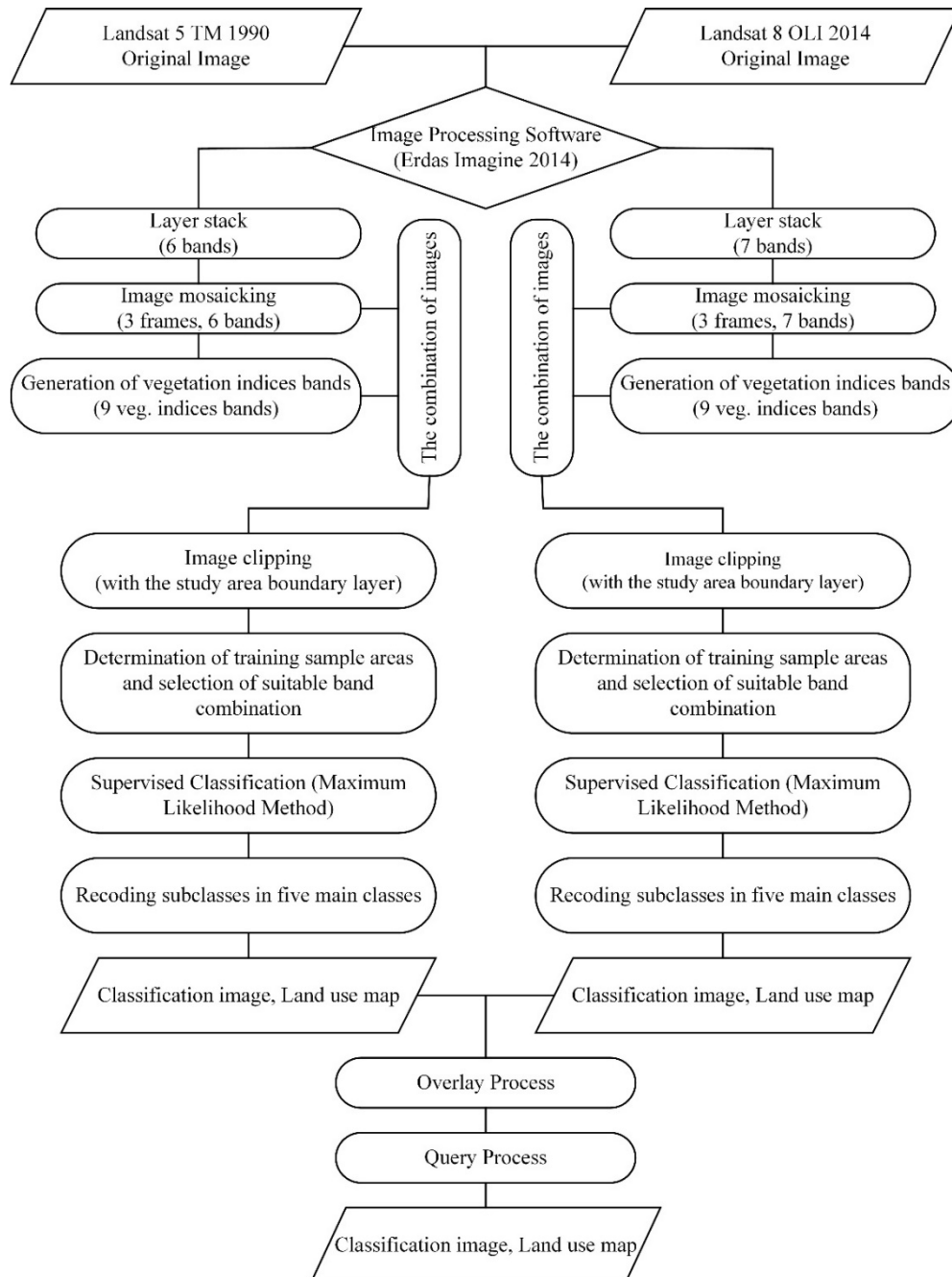*Bands 10 and 11 (TIRS 1 and TIRS 2) are resampled to 30 meters spatial resolution.

Figure 2. Flow chart of study

When image data is recorded by sensors aboard satellites and aircraft, errors may arise in geometry and the measured brightness values of pixels (Richards, 2013). The satellite images utilized in this study were downloaded in orthorectified form, thus obviating the necessity for geometric correction. Then, a mosaicking process was applied, which allows the merging of images consisting of several frames into a single image. In this stage, three full Landsat 5 TM images were used for the 1990, while three full Landsat 8 OLI images were used for the 2014. Histogram matching technique was employed during the mosaicking procedures. The primary purpose of utilizing this method is the calibration of the mosaic images. In this study, nine different vegetation indices were generated separately for Landsat 5 TM and Landsat 8 OLI images (Table 3). Subsequently, a new composite image, consisting of 15 bands with the six original bands of Landsat 5 TM images with the vegetation index images derived from these bands for the 1990 dataset, was created. Similarly, another new composite image consisting of 16 bands was generated by layer stacking of the seven original bands of Landsat 8 OLI with the indices created for the 2014 dataset. In the subsequent step, forest management plans pertaining to the study area were referenced in the ArcGIS program to delineate the study area boundaries in shapefile format. These boundaries were then converted to the AOI (Area of Interest) format using the ERDAS program. Then, the mosaic images from 1990 and 2014 were clipped to match the study area boundaries. To reduce their impact on classification, areas with dense cloud cover in the images were digitized into polygons and removed.

Table 3. Generated vegetation indices and their formulas

Index	Index description	Formula	Reference
DVI	Difference Vegetation Index	$NIR - Red$	(Tucker, 1979)
IR/R	Infrared divided by Red	IR/Red	(Jordan, 1969)
MSAVI2	Modified Soil Adjusted Vegetation Index 2	$((2NIR + 1 - \sqrt{(2NIR + 1)^2 - 8(NIR - Red)})/2$	(Qi et al., 1994)
NDVI	Normalized Difference Vegetation Index	$(NIR - Red)/(NIR + Red)$	(Rouse et al., 1974)
RDVI	Renormalized Difference Vegetation Index	$(NIR - Red)/\sqrt{(NIR + Red)}$	(Roujean and Breon, 1995)
RVI	Ratio Vegetation Index	Red/NIR	(Rondeaux et al., 1996)
SAVI	Soil Adjusted Vegetation Index	$(NIR - Red)(1 + L)/(NIR + Red + L)$ L=0.5 Vegetation Cover Correction Factor	(Huete, 1988)
SQRT(IR/R)	Square root of (Infrared/Red)	$\sqrt{(NIR/Red)}$	(Tucker, 1979)
TNDVI	Transformed Normalized Difference Vegetation Index	$\sqrt{((NIR - Red)/(NIR + Red)) + 0.5}$	(Deering et al., 1975)

2.3 Determination of land cover types and classification of images

With the addition of vegetation indices to the 1990 and 2014 images, the number of bands was increased to 16 and 17, respectively. Then, an unsupervised classification was conducted with varying numbers of classes to explore potential sub-information classes within the images with the ERDAS software. After forest management data was defined in the same projection system as the satellite data, the training data were created using the ArcGIS software. For the 1990 image, training data were defined using the unsupervised classification derived from the 1990 image, forest stand type maps from the 1992 forest management plans, and the 1990 Landsat 5 TM satellite image. When determining the training areas for the 2014 image, subclasses resulting from the unsupervised classification applied to the 2014 image, forest stand type maps from the 2013 forest management plans, the 2014 Landsat 8 OLI satellite image, and the high-resolution base map provided by ArcGIS online service were utilized. Five different land use classes were identified to classify the images obtained in 1990 and 2014 and detect changes. For representation of these classes, 434 training areas were selected from the 1990 image and 419 training areas from the 2014 image.

The training areas, each considered a separate subclass, were imported into the Erdas software and incorporated into the 'signature editor' section of the subclassification module. Spectral reflectance curves of vegetation indices were generated. Through the examination of these spectral reflectance curves, similar spectral classes were identified, and those mixed with others were determined. Upon evaluating the spectral reflectance curves, it was found that the DVI, IR/Red, and NDVI vegetation indices provided the highest differences. Thus, three vegetation indices derived using 6-band Landsat 5 TM sensor imagery and 7-band

Landsat 8 OLI sensor imagery were combined (bands were selected for classification based on signature analysis) to generate a 9-band image for 1990 (Blue, Green, Red, Near Infrared, Shortwave Infrared 1, Shortwave Infrared 2, DVI, IR/Red, NDVI) and a 10-band image (Coastal Aerosol, Blue, Green, Red, Near Infrared, Shortwave Infrared 1, Shortwave Infrared 2, DVI, IR/Red, NDVI). Then, supervised classification was applied to the images using the maximum likelihood algorithm.

The classification process advanced by recoding the sub-information classes into the 5 main information classes based on the objectives. The main land use classes were generated along with their corresponding code values (Table 4). The recoding process was carried out among classes with adjacency and the highest rate of inter-class mixture.

To ensure the validity of the classification, the accuracy assessment was performed using Erdas software. For the analysis, a total of 250 random ground control points (GCPs) were allocated, with 50 points assigned to each main information class for each year. The reference codes for the GCPs in 1990 were determined using Google Earth images and forest management plans. Forest management plans are prepared according to the act by the General Directorate of Forestry. A multi-layered approach is employed in the preparation of these plans. In brief, initial stand draft data is generated using aerial photographs, followed by ground measurements for sampling to create forest management plans (Mevzuat Bilgi Sistemi, 2024) For the determination of reference codes for the GCPs in 2014, satellite images, forest management plans, and a high-resolution base map were utilized. Subsequently, accuracy reports and error matrices for both years were obtained through the accuracy assessment module of the Erdas software.

Table 4. Major land use classes, where subclasses are combined, and their code values

Subclasses	Major land use classes	Code Values
Coniferous forests		
Deciduous forests		
Plantation areas	Forest areas	1
Coppice areas		
Maquis		
Cultivated agricultural areas		
Non-cultivated agricultural areas	Agricultural areas	2
Irrigated agricultural areas		
Residential areas		
Asphalt roads	Settlement areas	3
Airports		
Forest soil		
Pasture areas		
Sandy areas		
Rocky areas	Other non-forest areas	4
Mining areas		
Soil roads		
Sea		
Ponds	Water bodies	5
Dams		

3. Results and Discussion
3.1. Determination of changes in land cover types

The study aims to determine land use land cover changes using a post-classification comparison method with classified satellite images from 1990 and 2014. To accomplish this, a matrix operation was applied to the classified images in Erdas. The resulting image obtained from this application is shown in Figure 3. There is no general rule to determine the reliability of assessments obtained through remote sensing at which level of accuracy. However, it is generally assumed that classifications are considered accurate and reliable if the accuracy rate of assessments obtained through remote sensing is equal to or greater than 80%. In this study, the classification accuracies for both years exceed this threshold. The overall accuracy rates obtained for the classifications of 1990 and 2014 are 92.0% and 89.20%, respectively. Based on these results, the classification has achieved a sufficient level of accuracy and reliability.
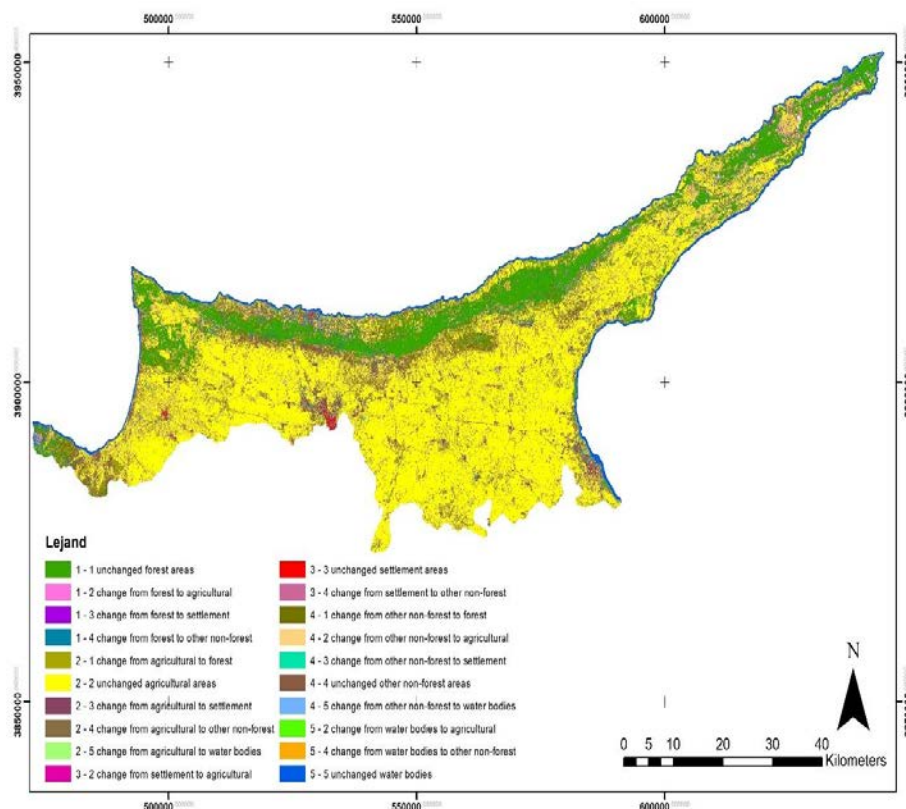

Figure 3. Thematic map depicting changes in land use forms between 1994 and 2000

Table 5 shows the classification results, their coverage for 1990 and 2014, along with the areal changes between the periods. The areal information for the codes in Figure 2 and the main information classes they represent can be found in Table 6. Specifically, codes such as 1-1, 2-2, 3-3, 4-4, 5-5 signify areas that remained unchanged between 1990 and 2014. Conversely, codes other than these signify inter-class changes in land use classes over the 24-year period.

Table 5. A comparison of land use classes between 1990 and 2014

Code	Class	Land use in 1990		Land use in 2014		Change (difference)	
		Area (ha)	Percent (%)	Area (ha)	Percent (%)	Area (ha)	Percent (%)
1	Forest	58236.91	17,00	69910.67	20.48	11673.76	3.41
2	Agricultural	226084.74	65.99	202551.91	59.12	-23532.83	-6.87
3	Settlement	2627.28	0.77	17891.6	5.15	15264.32	4.46
4	Other non-forest	45424,00	13.26	41901.21	12.23	-3522.79	-1.03
5	Water bodies	10226.07	2.98	10343.61	3.02	117.54	0.03
	Total	342599	100	342599	100		

Table 6. Changes occurring in land use classes between 1990 and 2014

Changing codes	Land use classes in 1990	Land use classes in 2014	Area (ha)	Percent (%)
1 - 1	Forest areas	Forest areas	45720,97	13,35
2 - 2	Agricultural areas	Agricultural areas	176221,00	51,44
3 - 3	Settlement areas	Settlement areas	1560,51	0,46
4 - 4	Other non-forest areas	Other non-forest areas	12161,80	3,55
5 - 5	Water bodies	Water bodies	10009,98	2,92
1 - 2	Forest areas	Agricultural areas	7724,07	2,25
1 - 3	Forest areas	Settlement areas	1252,08	0,37
1 - 4	Forest areas	Other non-forest areas	3539,79	1,03
1 - 5	Forest areas	Water bodies	0	0
2 - 1	Agricultural areas	Forest areas	13575,70	3,96
2 - 3	Agricultural areas	Settlement areas	10646,60	3,11
2 - 4	Agricultural areas	Other non-forest areas	25595,90	7,47
2 - 5	Agricultural areas	Water bodies	45,54	0,01
3 - 1	Settlement areas	Forest areas	0	0
3 - 2	Settlement areas	Agricultural areas	675,00	0,20
3 - 4	Settlement areas	Other non-forest areas	391,77	0,11
3 - 5	Settlement areas	Water bodies	0	0
4 - 1	Other non-forest areas	Forest areas	10614,00	3,10
4 - 2	Other non-forest areas	Agricultural areas	17927,70	5,23
4 - 3	Other non-forest areas	Settlement areas	4432,41	1,29
4 - 5	Other non-forest areas	Water bodies	288,09	0,08
5 - 1	Water bodies	Forest areas	0	0
5 - 2	Water bodies	Agricultural areas	4,14	0,00
5 - 3	Water bodies	Settlement areas	0	0
5 - 4	Water bodies	Other non-forest areas	211,95	0,06
	Total		342599	100

3.2. Examining the changes in land cover types

The research conducted within this study aimed to evaluate the expansion and contraction of land cover classes, particularly forest lands, both in terms of areal and spatial distribution. Subsequently, the causes of these changes were examined. When examining Table 6, it becomes evident that 71.72% of the total area exhibits no changes in land use classes, while changes are observed in 28.28% of the area. According to the change analysis results from 1990 to 2014, it was determined that the most significant change in the study area occurred in the transition from Agricultural Areas to Other non-forest

Areas, accounting for 7.47% of the total area. Upon examining transitions from one main information class to another, it was revealed that the most substantial change occurred in transitions from Agricultural Areas in 1990 to other main information classes, constituting 14.55% of the total area. Additionally, among all transitions from various main information classes in 1990, the most significant shift was toward the Other non-forest Areas class, which accounted for 8.67% of the total area.

When examining the spatio-temporal changes in forest areas, it is noted that despite two major forest fires occurring between 1990 and 2014 (the Great Besparmak Mountains Fire in 1995 and the Güzelyurt District Forestry Directorate Hacibayram I Series Fire in 1998) and a significant increase in population in the region, areas classified as forests have shown an increase of 3.41%. Reviewing Table 6 shows that an area of 1252.08 hectares has transitioned from Forest Areas to Settlement Areas. It can be said that these areas have irreversibly lost their forest quality.

When examining Table 5, a decrease of 6.87% is observed in Agricultural Areas. Upon reviewing Table 6, it is noted that an area of 25,595.90 hectares has transitioned from the Agricultural Areas main information class to the Other non-forest Areas main information class. In this transition, Agricultural Areas cultivated in 1990 were probably either harvested or left fallow by 2014.

Upon reviewing Tables 5 and 6, it is evident that there has been a significant increase of 4.46% in Settlement Areas. This main information class has experienced the highest transition from Agricultural Areas and Other non-forest Areas main information classes. The findings of this study highlight significant land cover changes in Cyprus between 1990 and 2014, characterized by the conversion of agricultural lands to other non-forest areas, alongside an increase in forest and settlement areas. These changes are consistent with patterns observed in other regions and underscore broader trends in land use dynamics.

Brown et al. (2005) utilized multi-temporal Landsat data to analyze urban sprawl in North America. They observed that urban expansion often displaces agricultural and natural areas, leading to notable environmental impacts. Our findings are analogous to those in Cyprus, where transitions from agricultural to urban land uses have also been observed.

Yong et al. (2003) employed Landsat-5 TM, Landsat-7 ETM+, and JERS-1 SAR data to study land cover changes and forest recovery in Changqing Forest Farm, Northeast China, following a 1987 forest fire. Their comparison of 1987 and 2000 Landsat images revealed successful forest and shrub land recovery from burn scars, alongside conversions to other land use types. Similarly, our study in Cyprus supports these findings, illustrating the effectiveness of afforestation and natural regeneration after wildfires.

The post-classification comparison method utilized in this study has been validated by various researchers for its robustness in detecting land cover changes (Bhattacharjee et al., 2021; Das and Angadi, 2022; Andualem et al., 2023; Thien and Phuong, 2023). Furthermore, Chungtai et al. (2021) conducted a comprehensive review of different change detection methods across diverse study areas, highlighting the unique applicability of the post-classification approach compared to other methods.

Tewabe and Fentahun (2020) focused on identifying land cover and land use changes in the Tana basin using Landsat data. Their findings underscored the critical role of change detection in monitoring land cover dynamics and devising strategies to mitigate adverse land use changes. This emphasizes the importance of continuous monitoring and the application of remote sensing techniques, as demonstrated in our study, for sustainable land management planning. In conclusion, the observed land cover changes in Cyprus between 1990 and 2014 reflect broader global trends. Using Landsat imagery and post-classification comparison methods has proven to be an effective approach for detecting these changes, providing essential insights into sustainable land management and planning.

4. Conclusions

The determination of temporal land cover changes, both spatial and areal, is essential for sustainable planning. In this study, satellite images acquired from different sensors for the years 1990 and 2014 were used to detect land cover changes in Cyprus. The results were evaluated using the post-classification comparison method. The overall classification accuracy for both years exceeded 85%. While these accuracy levels are considered sufficient, further improvement was constrained by the heterogeneous structure of the study area and low spectral separability among certain land cover classes. According to the change matrix analysis, land cover changes were observed across 96,924.74 hectares (28.28%) of the total 342,599-hectare study area, while no changes were detected in the remaining 245,674.26 hectares (71.72%). A decrease was identified in areas classified as agricultural land and other non-forest areas, whereas forest and settlement areas showed an increase. Water bodies exhibited minimal or no significant change. While forest management plans provide a snapshot of the current condition of forested areas, land cover change analyses offer insights into temporal dynamics, thereby facilitating more informed and effective planning. This study enhances the understanding of land use dynamics in Cyprus. Future research should prioritize the long-term monitoring of land use patterns, particularly in the context of climate change and natural resource sustainability. Additionally, comparative analyses across different regions and time periods may support the development of more comprehensive policy recommendations.

References

Andualem, T.G., Peters, S., Hewa, G.A., Boland, J., Myers, B.R. 2023. Spatiotemporal trends of urban-induced land use and land cover change and implications on catchment surface imperviousness. *Applied Water Science*, 13(12): 223. https://doi.org/10.1007/s13201-023-02029-7

Berberoglu, S., Akin, A. 2009. Assessing different remote sensing techniques to detect land use/cover changes in the eastern Mediterranean. *International Journal of Applied Earth Observation and Geoinformation*, 11(1): 46–53. https://doi.org/https://doi.org/10.1016/j.jag.2008.06.002

Bhattacharjee, S., Islam, M.T., Kabir, M.E., Kabir, M.M. 2021. Land-Use and Land-Cover Change Detection in a North-Eastern Wetland Ecosystem of Bangladesh Using Remote Sensing and GIS Techniques. *Earth Systems and Environment*, 5(2): 319–340. https://doi.org/10.1007/s41748-021-00228-3

Brown, D.G., Johnson, K. M., Loveland, T.R., Theobald, D.M. 2005. Rural land-use trends in the conterminous united states, 1950–2000. *Ecological Applications*, 15(6): 1851–1863.

CCRS. 2009. *Fundamentals of Remote Sensing*. Canada Center for Remote Sensing. 258 p.

Chungtai, A.H., Abbasi, H., Karaş, İ.R. 2021. A review on change detection method and accuracy assessment for land use land cover. *Remote Sensing Applications Society and Environment*, 22(2): 100482.

Çoban, H.O. 2006. Uydu Verileri ile Orman Alanlarındaki Zamansal Değişimlerin Belirlenmesi [Doctoral Thesis]. Istanbul Üniversity. Istanbul.

Das, S., Angadi, D.P. 2022. Land use land cover change detection and monitoring of urban growth using remote sensing and GIS techniques: a micro-level study. *GeoJournal*, 87(3): 2101–2123. https://doi.org/10.1007/s10708-020-10359-1

Deering, D.W., Rouse, J.W., Haas, R.H., Schell, J.A. 1975. Measuring "forage production" of grazing units from Landsat MSS data. 10th International Symposium on Remote Sensing of Environment, 1169–1178.

ESRI. 2024. *World Imagery*. Retrieved July 10, 2024, from https://www.arcgis.com/home/item.html?id=10df2279f9684e4a9f6a7f08febac2a9%3FWT.mc_id%3DEmailCampaign15361

Huete, A.R. 1988. A soil-adjusted vegetation index (SAVI). *Remote Sensing of Environment*, 25(3): 295–309. https://doi.org/10.1016/0034-4257(88)90106-X

Jensen, J.R. 1996. *Introductory Digital Image Processing: A Remote Sensing Perspective* (2nd Edition). Prentice Hall.

Jordan, C.F. 1969. Derivation of Leaf-Area Index from Quality of Light on the Forest Floor. *Ecology*, 50(4): 663–666.

Koç, A., Selik, C. 2004. Belgrad ormanında arazi kullanımının uzaktan algılama yöntemleri ile belirlenmesi. *Journal of the Faculty of Forestry Istanbul University*, 46(1): 137–146. https://doi.org/10.17099/jffiu.56773

Lu, D., Mausel, P., Brondízio, E., Moran, E. 2004. Change detection techniques. *International Journal of Remote Sensing*, 25(12): 2365–2401. https://doi.org/10.1080/0143116031000139863

Mas, J. 1999. Monitoring land-cover changes: A comparison of change detection techniques. *International Journal of Remote Sensing (IJRS)*, 20:139–152. https://doi.org/10.1080/014311699213659

Mevzuat Bilgi Sistemi. 2024. Orman Amenajman Yönetmeliği. Retrieved July 10, 2024, from https://www.mevzuat.gov.tr/mevzuat?MevzuatNo=11952&MevzuatTur=7&MevzuatTertip=5

Qi, J., Chehbouni, A., Huete, A.R., Kerr, Y.H., Sorooshian, S. 1994. A modified soil adjusted vegetation index. *Remote Sensing of Environment*, 48(2): 119–126. https://doi.org/10.1016/0034-4257(94)90134-1

Richards, J.A. 2013. Remote sensing digital image analysis: An introduction. In *Remote Sensing Digital Image Analysis: An Introduction* (5th ed, Vol.

9783642300622). Springer-Verlag Berlin Heidelberg. https://doi.org/10.1007/978-3-642-30062-2

Rondeaux, G., Steven, M., Baret, F. 1996. Optimization of soil-adjusted vegetation indices. *Remote Sensing of Environment*, 55(2), 95–107. https://doi.org/10.1016/0034-4257(95)00186-7

Roujean, J.L., Breon, F.M. 1995. Estimating PAR absorbed by vegetation from bidirectional reflectance measurements. *Remote Sensing of Environment*, 51(3): 375–384. https://doi.org/10.1016/0034-4257(94)00114-3

Rouse, J.W., Haas, R.H., Schell, J.A., Deering, D.W. 1974. Monitoring Vegetation Systems in The Great Plains with ERTS. Goddard Space Flight Center 3d Earth Resources Technology Satellite-1 Symposium, 309–317.

Roy, D.P., Wulder, M.A., Loveland, T.R., Allen, R.G., Anderson, M.C., Helder, D., Irons, J.R., Johnson, D.M., Kennedy, R., Scambos, T.A., Schaaf, C.B., Schott, J.R., Sheng, Y., Vermote, E.F., Belward, A.S., Bindschadler, R., Cohen, W.B., Gao, F., … Zhu, Z. 2014. Landsat-8: Science and product vision for terrestrial global change research. *Remote Sensing of Environment*, 145: 154–172. https://doi.org/10.1016/j.rse.2014.02.001

Sunar, F. 1998. An analysis of changes in a multi-date data set: A case study in the Ikitelli area, Istanbul, Turkey. *International Journal of Remote Sensing*, 19(2): 225–235. https://doi.org/10.1080/014311698216215

Tewabe, D., Fentahun, T. 2020. Assessing land use and land cover change detection using remote sensing in the Lake Tana Basin, Northwest Ethiopia. *Cogent Environmental Science,* 6(1): 1778998.

Thien, B.B., Phuong, V.T. 2023. Detection of Land Use and Land Cover Change Using Remote Sensing and GIS in Ba Ria-Vung Tau Province, Vietnam. *Geography and Natural Resources*, 44(4): 383–393. https://doi.org/10.1134/S1875372823040133

Tucker, C.J. 1979. Red and photographic infrared linear combinations for monitoring vegetation. *Remote Sensing of Environment*, 8(2): 127–150. https://doi.org/10.1016/0034-4257(79)90013-0

USGS. 2024. *What are the band designations for the Landsat satellites?* Retrieved July 10, 2024, from https://www.usgs.gov/faqs/what-are-band-designations-landsat-satellites

Yener, H., Koç, A. 2006. Monitoring changes in forest and other land use forms in Istanbul. *Journal of Environmental Biology*, 27(1): 77–83.

Yong, P., Sun, G., Zengyuan, L., Xuejian, C., Yanfang, D., Zhang, Z. 2003. Land cover change monitoring after forest fire in northeast China. *2003 IEEE International Geoscience and Remote Sensing Symposium Proceedings*, 3383–3385.